Comparative high-field magnetotransport of the oxypnictide superconductors $R\mathrm{FeAsO}_{1-x}\mathrm{F}_x$ (R=La, Nd) and $\mathrm{SmFeAsO}_{1-\delta}$

J. Jaroszynski, Scott C. Riggs, F. Hunte, A. Gurevich, D. C. Larbalestier, and G. S. Boebinger
National High Magnetic Field Laboratory, Florida State University, Tallahassee, Florida 32310, USA

F. F. Balakirev and Albert Migliori
National High Magnetic Field Laboratory, Los Alamos National Laboratory, Los Alamos, New Mexico 87545, USA

Z. A. Ren, W. Lu, J. Yang, X. L. Shen, X. L. Dong, and Z. X. Zhao
National Laboratory for Superconductivity, Institute of Physics and Beijing National Laboratory for Condensed Matter Physics, Chinese Academy of Sciences, P.O. Box 603, Beijing 100190, People's Republic of China

R. Jin, A. S. Sefat, M. A. McGuire, B. C. Sales, D. K. Christen, and D. Mandrus
Materials Science Division, Oak Ridge National Laboratory, P.O. Box 2008, Oak Ridge, Tennessee 37831, USA
(Received 13 June 2008; revised manuscript received 17 July 2008; published 12 August 2008)

We compare magnetotransport of the three iron-arsenide-based compounds ReFeAsO (Re=La, Sm, Nd) in very high DC and pulsed magnetic fields up to 45 and 54 T, respectively. Each sample studied exhibits a superconducting transition temperature near the maximum reported to date for that particular compound. While high magnetic fields do not suppress the superconducting state appreciably, the resistivity, Hall coefficient, and critical magnetic fields, taken together, suggest that the phenomenology and superconducting parameters of the oxypnictide superconductors bridges the gap between MgB_2 and YBCO.

DOI: 10.1103/PhysRevB.78.064511 PACS number(s): 74.70.−b, 74.25.Fy, 74.72.−h, 74.81.Bd

The recently discovered layered superconducting oxypnictides with high transition temperatures[1] are based on alternating structures of FeAs and ReO layers. Similar to the high-temperature superconducting cuprates, superconductivity in oxypnictides seem to emerge upon doping of a parent antiferromagnetic state. As the ReO planes are doped, the ionically bonded ReO donates an electron to the covalently bonded FeAs plane,[2] suppressing the global antiferromagnetism and resulting in superconductivity. Different rare earths do, however, have an effect on the superconducting transition temperature, T_c, which increases from a maximum of 28 K for La (Refs. 2 and 3) to above 40 K for Ce (Ref. 4) and above 50 K for Nd, Pr, Sm, and Gd, respectively.[5–8] Unlike the cuprates, the doping required for the onset of superconductivity, as well as the doping at optimal T_c, seems to depend on the specific rare earth in the compound, perhaps for intrinsic reasons such as a varying the magnetic moment or size of the rare-earth atom, or a possible role of multiple bands.

To deduce common behaviors of the oxypnictide superconductors, we studied three of the iron-arsenide-based compounds ReFeAsO (Re=La, Sm, Nd) in very high magnetic fields. All samples measured were polycrystals made by solid-state synthesis. Two were doped by partial F substitution for O (La and Nd) and one (Sm) by forcing an O deficiency. The $\mathrm{SmFeAsO}_{0.85}$ (Ref. 9) and $\mathrm{NdFeAsO}_{0.94}\mathrm{F}_{0.06}$,[5] exhibiting a 90% $T_c \approx 53.5$ and ≈ 50.5 K, respectively, were grown at the National Laboratory for Superconductivity in Beijing. These samples result from high-pressure synthesis. SmAs (or NdAs) presintered powder and Fe, Fe_2O_3, and FeF_2 powders were mixed together according to the nominal stoichiometric ratio then ground thoroughly and pressed into small pellets. The pellets were sealed in boron nitride crucibles and sintered in a high-pressure synthesis apparatus under a pressure of 6 GPa at 1250 °C for 2 h. The $\mathrm{LaFeAsO}_{0.89}\mathrm{F}_{0.11}$ sample from the Oak Ridge group has $T_c \approx 28$ K,[3] which is among the highest transition temperatures reported for this compound at ambient pressure.[2] It was grown by a standard solid-state synthesis method similar to that reported previously,[1] from elements and binaries, with purity >4 N. Our extensive studies on morphology, connectivity, electromagnetic granularity, phase purity, magnetic properties etc. could be find elsewhere.[10–12]

Phase diagrams for fluorine-doping[1,13,14] have been reported for each compound: our $\mathrm{LaFeAsO}_{0.89}\mathrm{F}_{0.11}$ and $\mathrm{SmFeAsO}_{0.85}$ samples are deemed optimally doped based upon the maximal value of T_c in the published F-doped phase diagrams, which is consistent with the nominal F-doping level for our samples.[1,13,14] It is important to note, however, that the actual doping of polycrystalline samples can be difficult to determine precisely. For example, the nominal doping of $x=0.06$ in our $\mathrm{NdFeAsO}_{0.94}\mathrm{F}_{0.06}$ sample is anomalously low in light of the published phase diagram, for which an experimental value of $T_c=50.5$ K corresponds to the maximum value of T_c, which is reported to occur at an F doping of around 11%. However, in contrast to the cuprates, the optimal doping range for these superconductors is wide. On the other hand, from technological point of view, it is often that the real F content is much smaller than the nominal for the ambient-pressure sintered samples, since lots of F was observed to react with quartz glass. However, we observe rather higher then nominal doping, probably because our Nd sample was high pressure sintered. This method has a better doping effect, in contrast to ambient-pressure samples which were used for the construction of the phase diagram.[14] Despite the uncertainty in doping levels, we believe that all

three of our samples are near optimal doping, because they exhibit transition temperatures very near the consensus values of highest T_c for these compounds at ambient pressure.

The longitudinal resistivity ρ_{xx} and the Hall coefficient R_H in high magnetic fields were measured using a lock-in technique in three different high-field magnets at the National High Magnetic Field Laboratory (NHMFL): 33 T DC resistive and 45 T hybrid magnets at Florida State University, and 54 T pulsed magnets at Los Alamos National Laboratory. For each experiment, the samples were nominally rectangular prisms and the magnetic field was applied perpendicular to the largest face of the samples. Six electrical contacts (using either DuPont silver paint or Epo-tek H20 E silver epoxy) were positioned around the perimeter of the sample in a conventional Hall bar geometry.

Figure 1(a) shows ρ_{xx} as a function of temperature T at $B=0$ for the $LaFeAsO_{0.89}F_{0.11}$, $SmFeAsO_{0.85}$, and $NdFeAsO_{0.94}F_{0.06}$ samples. $LaFeAsO_{0.89}F_{0.11}$ exhibits a conventional superlinear T dependence of $\rho_{xx}(T)$. A magnetic field suppresses superconductivity by shifting the resistive transition to lower T, reducing T_c by roughly a factor of two with 30 T, as shown in Fig. 1(b).

$SmFeAsO_{0.85}$ and $NdFeAsO_{0.80}F_{0.06}$ show strikingly different behavior that is more reminiscent of the high-temperature superconducting cuprates: a linear temperature dependence of $\rho_{xx}(T)$, from 225 K down to T_c and a substantial broadening of the resistive transition in a magnetic field: applying 33 T has little effect on the high-temperature superconductivity onset, while the foot of the transition is shifted to substantially lower temperature as shown in Figs. 1(c) and 1(d).

The field dependencies of the Hall resistivity ρ_{xy} are shown in Figs. 2(a)–2(c) for the La, Sm, and Nd compounds, respectively, over a wide temperature range above T_c. The low-temperature behavior of the La compound at $T<100$ K in Fig. 2(a) is rather conventional: ρ_{xy} is linear in B and is temperature independent. If only one band contributes to current transport, the Hall coefficient, $R_H=\rho_{xy}/B=1/ne$, yields a carrier density n of 0.07 electrons per unit formula in the La compound at low temperatures. Here we used reported unit-cell parameters[15] with two unit formulas per unit cell. This value is not far from the nominal doping of $x=0.1$ per unit formula.

At higher T all three compounds exhibit a strong temperature dependence of ρ_{xy} as is evident in Figs. 2(a)–2(c). Note, however, that all traces in Fig. 2 retain a linear dependence on B regardless of temperatures. The observed strictly linear field dependence of ρ_{xy} and no magnetoresistance at temperatures 70–200 K indicates that $\omega_c\tau \ll 1$, where $\omega_c=eB/m^*$ is the cyclotron frequency and τ is the scattering time. At the same time the observed temperature dependence of R_H may indicate two-band effects.

A number of experimental[16–18] and theoretical[19–21] papers have discussed the oxypnictides as a two-band system. In this case, the primary effect of high magnetic fields is the lateral separation of electronlike and holelike carriers. Often ρ_{xy} for a semimetal is not a linear function of H due to the complexity of the transport in the presence of two different carriers. The field dependence of R_H for a two-band system[22]

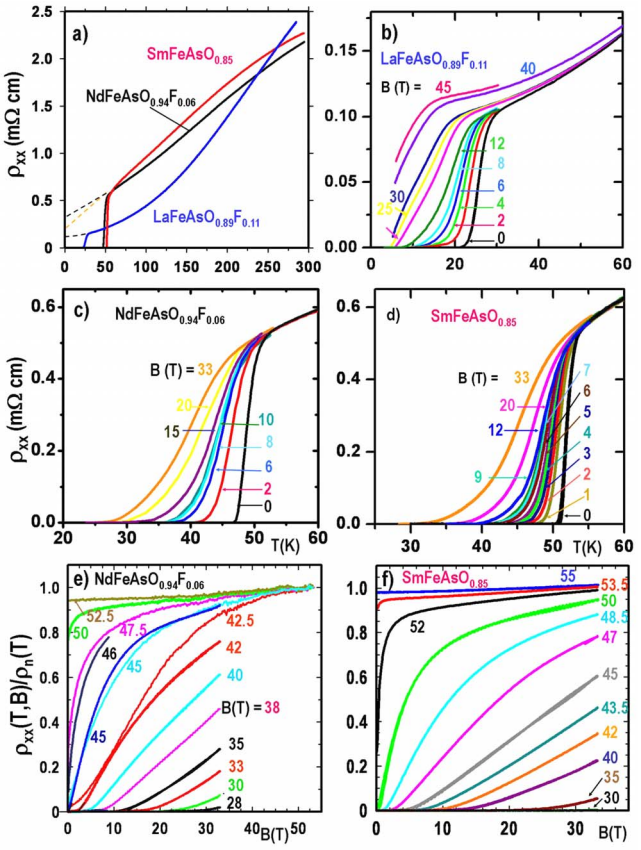

FIG. 1. (Color online) (a) Longitudinal resistivity $\rho_{xx}(T)$ at $B=0$ for three members of the $ReO_{1-x}F_xFeAs$ system: $LaFeAsO_{0.89}F_{0.11}$ with $T_c \simeq 28$ K, $SmFeAsO_{0.85}$ with $T_c \simeq 53.5$ K, and $NdFeAsO_{0.94}F_{0.06}$ with $T_c \simeq 50.5$ K. Dashed lines show normal resistance $\rho_n(T)$ extrapolated below T_c. (b) ρ_{xx} at various magnetic fields as a function of temperature for La compound at $B=0$, 2, 4, 6, 8, 12, 20, 25, 30, 40, and 45 T; (c) Nd compound at $B=0$, 2, 6, 8, 10, 15, 20, and 33 T; and (d) for Sm compound at $B=0$, 1, 2, 3, 4, 5, 6, 7, 8, 9, 12, 25, and 33 T. (e) Normalized resistivity $\rho_{xx}(B,T)/\rho_n(T)$ of Nd sample vs B at various T measured in dc resistive magnet up to 33 T (sweep rate 5 T/min) and pulsed magnetic field up to 54 T. The latter data exhibit saturation at lower temperatures which may result from eddy current heating in this relatively big sample. (f) $\rho_{xx}(B,T)/\rho_n(T)$ of Sm sample versus B at various T measured in dc resistive magnet up to 33 T.

$$R_H = \frac{\sigma_1^2 R_1 + \sigma_2^2 R_2 + \sigma_1^2\sigma_2^2 R_1 R_2 (R_1+R_2) B^2}{(\sigma_1+\sigma_2)^2 + \sigma_1^2\sigma_2^2 (R_1+R_2)^2 B^2} \quad (1)$$

becomes noticeable as the parameter $\omega_c\tau = B/B_0$ becomes of the order of unity provided that $R_1 \sim R_2$ and $\sigma_1 \sim \sigma_2$. Here $B_0=\rho_{xx}/R_H$, the indices 1 and 2 correspond to bands 1 and 2, $R_{1,2}$ and $\sigma_{1,2}=1/\rho_{1,2}$ are intraband Hall coefficients and conductivities, respectively, and ρ_{xx} is determined by the minimum value of ρ_1 and ρ_2 in the parallel band connection. Taking the characteristic values of $\rho_{xx} \simeq 1$ m Ω cm and $R_H \simeq 5\times 10^{-3}$ cm^3/C from Figs. 1 and 2, we get $B_0=2000$ T, indicating that $\omega_c\tau \gg 1$ only at inaccessible magnetic fields $H>1000$ T. The same field B_0 sets the scale for the onset of magnetoresistance. Note that in Fig. 1, there is no significant

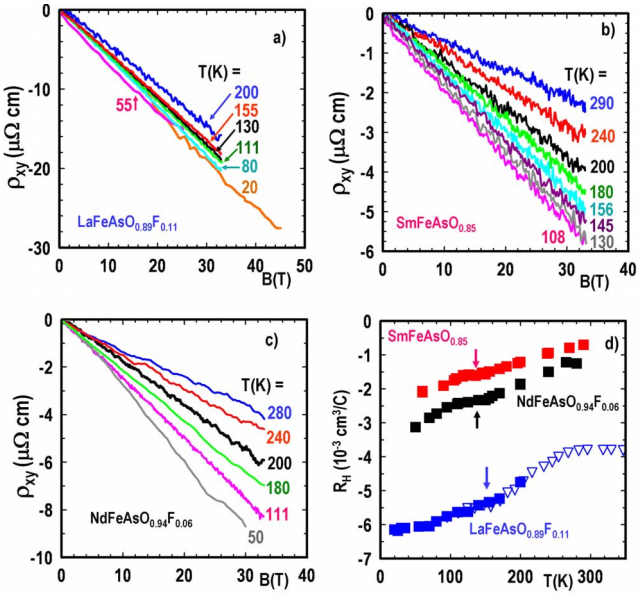

FIG. 2. (Color online) The Hall resistivity ρ_{xy} versus magnetic field for: (a) La compound, (b) Sm compound and (c) Nd compound at $T > T_c$. Note that all ρ_{xy} show a linear dependence on magnetic field. The low-temperature ρ_{xy} for the La compound are also temperature independent, consistent with a dominant single-carrier conduction mechanism, while at higher T all compounds show marked $\rho_{xy}(T)$ dependencies. (d) Hall coefficient determined from linear fits to $\rho_{xy}(H)$ for $-33 < B < 33$ T or $11.5 < B < 45$ T (solid squares) and at $B = 9$ T (open triangles Ref. 3). No systematic departure from linearity was found regardless of temperature. Arrows show apparent inflections on $R_H(T)$ dependence around $T \approx 150$ K, which may result from structural transitions.

magnetoresistance above T_c, where the zero-field data (black line) superimpose data taken in magnetic fields. Thus, the observed temperature dependence of R_H is consistent with a two-band system at $\omega_c \tau \ll 1$ for both bands with no visible magnetoresistance and the Hall resistivity $\rho_{xy} = B(\sigma_1^2 R_1 + \sigma_2^2 R_2)/(\sigma_1 + \sigma_2)^2$ linear in B.

Figure 2(d) shows the marked temperature dependencies of R_H, which exhibit pronounced inflections at temperatures marked by the three arrows. These arrows indicate the temperatures at which a structural phase transition has been reported for the three *undoped* parent compounds. Neutron data on undoped LaFeAsO show a transition from tetragonal to monoclinic lattice around 150 K, followed by antiferromagnetic ordering below 134 K.[23] SmFeAsO shows a tetragonal to orthorhombic transition at 129 K.[24] For NdFeAsO, sharp jumps in heat-capacity signal structural transition at ≈ 150 K.[25] Unlike the pseudogap in the cuprates, doping of the parent compound only slightly reduces the temperature of these anomalies in the oxypnictides as the doping approaches the range in which superconductivity is observed.[1,13,14] The Hall data in Fig. 2 suggest that a remnant of the structural transitions in the undoped parent compounds manifest themselves at optimum doping as well; however, it is also possible that this results from the presence of undoped phase in the samples. At the same time, the overall temperature dependence of $R_H(T)$ is not understood.

Finally, the high-field longitudinal resistivity measurements shown in Fig. 1 enable a characterization of the magnetic-field scales required to suppress superconductivity in the oxypnictides. Figure 3 shows three characteristic fields $H_{90}(T)$, $H_{50}(T)$, and $H_{10}(T)$ at which $\rho_{xx}(T)$ reaches 90%, 50%, and 10% of the normal-state resistivity $\rho_n(T)$ extrapolated linearly from its temperature dependence above T_c. For all three compounds, the data in Fig. 3 are reminiscent of the quasi-two-dimensional (quasi-2D) layered cuprate superconductors.[26] Following a previous analysis for polycrystalline samples,[16] we assume that, because of the strong angular dependence of $H_{c2}(\theta)$, the field $H_{10}(T)$ scales like $H_{c2}^{\perp}$ parallel to the c axis, that is, the geometry for which the magnetic field most readily suppresses the superconducting state. The resistivity $\rho_{xx}(T,H)$ at the very bottom of the transition, say at $0.5\%\rho_n$ matches the onset of the pinned critical state of vortices below the irreversibility field $H_{\rm irr}(T)$ extracted from magnetization measurements.[10] The 90% data in turn likely corresponds to $H_{c2}(T)$ perpendicular to the c axis, as only at this point has superconductivity been largely suppressed for all orientations of the polycrystalline grains.

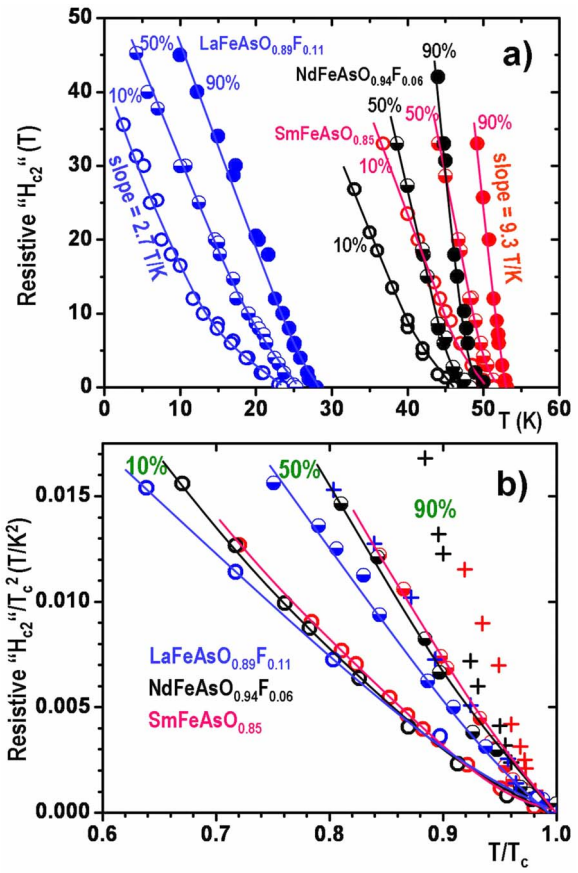

FIG. 3. (Color online) (a) Upper critical fields H_{c2} versus temperature for the Sm, Nd, and La compounds. with $T_c = 53.5$, 50.5, and 28 K respectively, as determined from 90% transitions; $T_c = 52$, 47.5, and 25 K for 50% transitions and $T_c = 51$, 46, and 23 K for 10% transitions. The data extracted from the results shown in Fig. 1 show the temperatures at which the resistance reaches 10%, 50%, and 90% of the normal-state resistance, as extrapolated linearly from the $\rho_n(T)$ temperature dependence above T_c. The solid lines guide the eye. (b) The same data divided by T_c^2 and plotted as a function of reduced temperature T/T_c.

Shown in Fig. 3(b) are the magnetic fields $H_{90}(T)$, $H_{50}(T)$, and $H_{10}(T)$ normalized to the respective values of T_c^2 for each compound and plotted as functions of the reduced temperature $t=T/T_c$. All $H_{50}(T)$ and $H_{10}(T)$ data nearly collapse onto single curves, while the $H_{90}(T)$ data do not. This behavior suggests the following qualitative interpretation. The upper critical fields $H_{c2}^{\perp}\sim\phi_0/2\pi\xi_a^2$ along the c axis and perpendicular to the c axis, $H_{c2}^{\parallel}\sim\phi_0/2\pi\xi_a\xi_c$ are defined by the respective coherence lengths, ξ_a and $\xi_c\simeq\xi_a\Gamma^{-1/2}$, where $\Gamma=\rho_c/\rho_{ab}$ is the effective mass or resistivity anisotropy parameter. Given the nanoscale ξ_a and ξ_c in oxypnictides,[16] we can assume that these materials even in the present polycrystalline form are likely in the clean limit, $\xi_a<\ell$, where ℓ is the mean-free path. In this case $\xi_a\propto\xi_c\propto 1/T_c$, which yields $H_{c2}\propto T_c^2$, consistent with the scaling of $H_{50}(T)$ and $H_{10}(T)$ curves defined by $H_{c2}^{\perp}$ in Fig. 3(b) for all three compounds. In turn, the lack of scaling for $H_{90}(T)$ defined by $H_{c2}^{\parallel}(T)$ in Fig. 3(b) may indicate that, in addition to the change in T_c, the mass anisotropy parameter Γ also changes, as will be discussed below.

Our high-field data enable us to make several further conclusions regarding trends in superconducting oxypnictides. From the measured $R_H=1/ne$ and the London penetration depth $\lambda_0^2=m^*/\mu_0 ne^2$ at $T=0$, we estimate the effective mass of the carriers $m^*=\mu_0 e\lambda_0^2/R_H$, where e is the electron charge. Taking $R_H=6.2\times10^{-3}$ cm^3/C at T_c from Figs. 1 and 2 and $\lambda_0=215$ nm from NMR data,[27] we obtain $m^*=1.6m_e$ for LaFeAs(O,F) (or a slightly higher $m^*=2.23m_e$ for $\lambda_0=254$ nm taken from μSR data[28]). For SmFeAsO, we take $R_H=2\times10^{-9}$ m^3/C from Fig. 2 and $\lambda_0=184$ nm from μSR data,[29] which yields $m^*=3.7m_e$. The increase of m^* as T_c increases from 28 K for LaFeAs(O,F) to 53.5 K for SmFeAsO may reflect the effective-mass renormalization by strong-coupling effects.[30] The above one band estimate can also be applied qualitatively to two-band systems, in which either the ratios m_1/n_1 and m_2/n_2 are not too different, or $\sigma_1\gg\sigma_2$. In the latter case m^* corresponds to band 1, which effectively short-circuits band 2. In turn, the ratio σ_1/σ_2 can be controlled by disorder, as has been shown for MgB_2.[31]

The relative effects of vortex fluctuations can be inferred from the data of Fig. 1. As mentioned previously, the $R(T)$ curve for LaFeAs(O,F) mostly shifts to lower temperatures without much change in shape upon increasing H. This behavior is characteristic of the resistive transition in low-T_c superconductors with weak thermal fluctuations of vortices. By contrast, the $R(T)$ curves for the higher-T_c oxypnictides in Figs. 1(c) and 1(d) broaden significantly as H increases, similar to the behavior of the cuprates. This indicates that thermal fluctuations of vortices in SmFeAsO and NdFeAs(O,F) appear to be much stronger than in LaFeAs(O,F). The effect of thermal fluctuations is quantified by the Ginzburg parameter, $Gi=(2\pi k_B T_c\mu_0\lambda_0^2/\phi_0^2\xi_c)^2/2$, $\xi_c=\xi_a\Gamma^{-1/2}$ is the coherence length along the c axis, $\Gamma=m_c/m_a$ is the mass anisotropy parameter in a uniaxial crystal.[32]

For LaFeAs(O,F), ξ_c can be estimated from the zero-temperature $H_{c2}^{\parallel}(0)=\phi_0/2\pi\xi_a\xi_c$, which yields $\xi_c=[\phi_0/2\pi H_{c2}^{\parallel}(0)\sqrt{\Gamma}]^{1/2}=1.2$ nm for $\Gamma=15$(Ref. 33) and $H_{c2}^{\parallel}(0)=60$ T.[16] In this case $Gi=3.4\times10^{-4}$ is only 50% higher than $Gi=2.1\times10^{-4}$ of clean MgB_2 [$T_c=40$ K, $\xi_a=5$ nm, $\Gamma=36$, and $\lambda_a/\xi_a=25$(Ref. 34)], but some are 30 times smaller than Gi for the least anisotropic cuprate, $YBa_2Cu_3O_{7-x}$.[32] Since ξ is inversely proportional to T_c, the slope $dH_{c2}^{\parallel}/dT\propto T_c\Gamma^{1/2}$ near T_c in the clean limit increases as T_c and Γ increase. The values of $dH_{c2}^{\parallel}/dT$ estimated from the slopes of $H_{90}(T)$ in Fig. 3 increase from 2.7 T/K for LaFeAs(O,F) to 9.3 T/K for SmFeAsO, indicating that SmFeAsO is more anisotropic with $\Gamma\sim15(9.3T_c^{\mathrm{La}}/2.7T_c^{\mathrm{Sm}})^2\simeq65$, which exceeds the anisotropy parameter $\Gamma\sim25-50$ of YBCO. This estimate is very close to $\Gamma\approx64$ at T_c inferred from the recent torque magnetic measurements on SmFAs(O,F) single crystals, which also revealed a temperature dependence of $\Gamma(T)$ indicative of two-band superconductivity.[35] The impact of high anisotropy on the Ginzburg parameter for SmFeAsO is large: $Gi^{\mathrm{Sm}}/Gi^{\mathrm{La}}=(T_c^{\mathrm{Sm}}\lambda_0^{\mathrm{Sm}}/T_c^{\mathrm{La}}\lambda_0^{\mathrm{La}})^4(\Gamma_{\mathrm{Sm}}/\Gamma_{\mathrm{La}})\simeq35$ and Gi^{Sm} is thus of the same order as Gi for YBCO. Our conclusions are also consistent with the recent measurements of H_{c2} on NdFeAs(O,F) single crystals, for which $dH_{c2}^{\parallel}/dT=9$ T/K, $dH_{c2}^{\perp}/dT=1.85$ T/K, $\xi_a\simeq1.85$ nm, $\xi_c\simeq0.38$ nm, and $\Gamma\simeq20-40$ depending on the sample purity.[36] These values of ξ are close to those for YBCO. Moreover, taking $\lambda_0=200$ nm, $\xi_c=0.38$ nm and $T_c=49$ K, we again obtain $Gi\simeq10^{-2}$, a typical Ginzburg number for YBCO. For two-band superconductors, the above estimates of Gi remain qualitatively the same if Γ and ξ are taken for the band with the minimum effective mass or maximum electron mobility.[31]

The relatively small value of Gi in the La compound indicates that the melting field of the vortex lattice, $H_m(T)$ is not too different from H_{c2}.[16] However, for Sm and Nd compounds, the difference between H_m and $H_{c2}^{\perp}$ becomes more pronounced because of the much larger Ginzburg numbers. In this case $H_m\ll H_{c2}$, even for a moderately anisotropic superconductor, for which

$$H_m=aH_{c2}(0)\frac{T_c^2}{T^2}\left(1-\frac{T}{T_c}\right)^2. \tag{2}$$

Here $a=\pi^2c_L^4/Gi$, and $c_L\approx0.17$ is the Lindemann number for the vortex lattice.[32] Taking the above-estimated value of $Gi\sim1.3\times10^{-2}$ for SmFeAsO, we obtain $a\sim0.63$. Here the melting field H_m(T) exhibits an upward curvature near T_c where H_m(T) is significantly smaller than $H_{c2}(T)\approx H_{c2}(0)(1-t)$. At lower temperatures $H_m(T)$ crosses over with $H_{c2}(T)$ in the same way as in cuprates.[32]

In conclusion, we have measured magnetotransport in three of the rare-earth oxypnictide superconductors: $LaFeAsO_{0.89}F_{0.11}$, $SmFeAsO_{0.85}$, and $NdFeAsO_{0.94}F_{0.06}$. From resistivity, Hall coefficient and upper critical magnetic fields, we conclude that $LaFeAsO_{0.89}F_{0.11}$ behaves as an intermediate-T_c superconductorlike MgB_2 in which thermal fluctuations of vortices do not significantly affect the H-T diagram to the extent that they do in the layered cuprates. However, the situation is different for the higher T_c oxypnictides, SmFeAsO, and NdFeAs(O,F), which exhibit a larger mass anisotropy, enhanced thermal fluctuations, and for which the Ginzburg parameter becomes comparable to that of YBCO. Thus, the series of oxypnictide superconductors bridges a conceptual gap between conventional superconductors and the high-temperature cuprates. As such, they hold particular promise for understanding the many still-

unexplained behaviors of the high-T_c cuprates.

The work at NHMFL was supported by the NSF Cooperative Agreement No. DMR-0084173, by the State of Florida, by the DOE, by the NHMFL IHRP program (FH), and by AFOSR Grant No. FA9550–06–1-0474 (AG and DCL). Work at ORNL was supported by the Division of Materials Science and Engineering, Office of Basic Energy Sciences.

[1] Y. Kamihara, T. Watanabe, M. Hirano, and H. Hosono, J. Am. Chem. Soc. **130**, 3296 (2008).
[2] H. Takahashi, K. Igawa, K. Arii, Y. Kamihara, M. Hirano, and H. Hosono, Nature (London) **453**, 376 (2008).
[3] A. S. Sefat, M. A. McGuire, B. C. Sales, R. Jin, J. Y. Howe, and D. Mandrus, Phys. Rev. B **77**, 174503 (2008).
[4] G. F. Chen, Z. Li, D. Wu, G. Li, W. Z. Hu, J. Dong, P. Zheng, J. L. Luo, and N. L. Wang, Phys. Rev. Lett. **100**, 247002 (2008).
[5] Z.-A. Ren *et al.*, Europhys. Lett. **82**, 57002 (2008).
[6] Z.-A. Ren, J. Yang, W. Lu, W. Yi, G.-C. Che, X.-L. Dong, L.-L. Sun, and Z.-X. Zhao, Mater. Res. Innovations **12**, 1 (2008).
[7] X. H. Chen, T. Wu, G. Wu, R. H. Liu, H. Chen, and D. F. Fang, arXiv:0803.3603 (unpublished).
[8] J. Yang *et al.*, Supercond. Sci. Technol. **21**, 082001 (2008).
[9] Z.-A. Ren *et al.*, Chin. Phys. Lett. **25**, 2215 (2008).
[10] A. Yamamoto *et al.*, Supercond. Sci. Technol. **21**, 095008 (2008).
[11] A. Yamamoto *et al.*, Appl. Phys. Lett. **92**, 252501 (2008).
[12] T. Fumitake (private communication).
[13] R. H. Liu *et al.*, arXiv:0804.2105 (unpublished).
[14] G. F. Chen, Z. Li, D. Wu, J. Dong, G. Li, W. Z. Hu, P. Zheng, J. L. Luo, and N. L. Wang, Chin. Phys. Lett. **25**, 2235 (2008).
[15] G. Giovannetti, S. Kumar, and J. van den Brink, arXiv:0804.0866, Physica B (to be published).
[16] F. Hunte, J. Jaroszynski, A. Gurevich, D. C. Larbalestier, R. Jin, A. S. Sefat, M. A. McGuire, B. C. Sales, D. K. Christen, and D. Mandrus, Nature (London) **453**, 903 (2008).
[17] Y. Wang, L. Shan, L. Fang, P. Cheng, C. Ren, and H.-H. Wen, arXiv:0806.1986 (unpublished).
[18] K. Matano, Z. A. Ren, X. L. Dong, L. L. Sun, Z. X. Zhao, and G. qing Zheng, Europhys. Lett. **83**, 57001 (2008).
[19] F. Ma and Z.-Y. Lu, Phys. Rev. B **78**, 033111 (2008).
[20] S. Raghu, X. L. Qi, C. X. Liu, D. J. Scalapino, and S. C. Zhang, Phys. Rev. B **77**, 220503(R) (2008).
[21] Q. Han, Y. Chen, and Z. D. Wang, EPL **82**, 37007 (2008).
[22] C. Kittel, *Introduction to Solid State Physics* (Wiley, New York, 2004).
[23] C. de la Cruz *et al.*, Nature (London) **453**, 899 (2008).
[24] C. Wiebe and H. Zhou (private communication).
[25] M. Fratini *et al.*, Supercond. Sci. Technol. **21**, 092002 (2008).
[26] Y. Ando, G. S. Boebinger, A. Passner, L. F. Schneemeyer, T. Kimura, M. Okuya, S. Watauchi, J. Shimoyama, K. Kishio, K. Tamasaku, N. Ichikawa, and S. Uchida, Phys. Rev. B **60**, 12475 (1999).
[27] K. Ahilan, F. L. Ning, T. Imai, A. S. Sefat, R. Jin, M. McGuire, B. Sales, and D. Mandrus, arXiv:0804.4026 (unpublished).
[28] H. Luetkens *et al.*, arXiv:0804.3115 (unpublished).
[29] A. J. Drew *et al.*, arXiv:0805.1042 (unpublished).
[30] I. I. Mazin, D. J. Singh, M. D. Johannes, and M. H. Du, arXiv:0803.2740 (unpublished).
[31] A. Gurevich, Physica C **456**, 160 (2007); Phys. Rev. B **67**, 184515 (2003).
[32] G. Blatter, M. V. Feigel'man, V. B. Geshkenbein, A. I. Larkin, and V. M. Vinokur, Rev. Mod. Phys. **66**, 1125 (1994).
[33] D. J. Singh and M.-H. Du, Phys. Rev. Lett. **100**, 237003 (2008).
[34] P. Canfield, S. Bud'ko, and D. Finnemore, Physica C **385**, 1 (2003).
[35] S. Weyeneth, U. Mosele, N. Zhigadlo, S. Katrych, Z. Bukowski, J. Karpinski, S. Kohout, J. Roos, and H. Keller, arXiv:0806.1024 (unpublished).
[36] Y. Jia, Y. Cheng, L. Fang, H. Luo, H. Yang, C. Ren, L. Shan, and H. Wen, arXiv:0806.0532 (unpublished).